



# IJRASET

International Journal For Research in  
Applied Science and Engineering Technology



---

# INTERNATIONAL JOURNAL FOR RESEARCH

IN APPLIED SCIENCE & ENGINEERING TECHNOLOGY

---

**Volume: 11    Issue: VIII    Month of publication: Aug 2023**

**DOI: <https://doi.org/10.22214/ijraset.2023.55280>**

**[www.ijraset.com](http://www.ijraset.com)**

**Call:  08813907089**

**E-mail ID: [ijraset@gmail.com](mailto:ijraset@gmail.com)**

# Spectral and Up conversion Properties of $\text{Ho}^{3+}$ ions doped Zinc Lithium Lead Soda lime Cadmium Phosphate Glasses

Dr. S. L. Meena

Ceramic Laboratory, Department of physics, Jai Narain Vyas University, Jodhpur 342001(Raj) India

**Abstract:** Glasses samples containing  $\text{Ho}^{3+}$  in zinc lithium lead sodalime cadmium phosphate  $(35-x)\text{P}_2\text{O}_5:10\text{ZnO}:10\text{Li}_2\text{O}:10\text{PbO}:10\text{CaO}:10\text{Na}_2\text{O}:15\text{CdO}:x\text{Ho}_2\text{O}_3$  (where  $x=1, 1.5, 2$  mol %) have been prepared by melt-quenching method. The amorphous nature of the prepared glass samples was confirmed by X-ray diffraction. Optical absorption, Excitation and fluorescence spectra were recorded at room temperature for all glass samples. Judd-Ofelt intensity parameters  $\Omega_\lambda$  ( $\lambda=2, 4$  and 6) are evaluated from the intensities of various absorption bands of optical absorption spectra. Using these intensity parameters various radiative properties like spontaneous emission probability (A), branching ratio ( $\beta$ ), radiative life time ( $\tau_R$ ) and stimulated emission cross-section ( $\sigma_p$ ) of various emission lines have been evaluated.

**Keywords:** ZLLSLCP Glasses, Optical Properties, Judd-Ofelt Theory, Upconversion Properties.

## I. INTRODUCTION

Rare earth doped glasses have attracted a great deal of attention because of their applications in thermal imaging, fiber amplifiers, laser fusion, optical fibers, photovoltaic solar cells, optical communications, up-conversion lasers and optical data storage [1–5]. Among different glasses, phosphate glasses have unique properties. They have high transparency, high thermal stability, optical stability and low phonon energy. Phosphate glasses possess excellent physicochemical properties, optical properties, lower phonon energy, better color rendering index(CRI), and low melting temperature [6-10]. The low nonlinear dispersion of the highly rare earth doped phosphate glasses enables there in high power applications. The low glass melting temperature makes the phosphate glasses suitable candidates for photonic applications. Phosphate glasses also exhibit high rare earth solubility [11,12]. Addition of network modifier (NWF)  $\text{Li}_2\text{O}$  to the phosphate glasses improves both electrical and mechanical properties of such glasses [13]  $\text{ZnO}$  is also added due to its specific chemical and microstructure properties. Addition of  $\text{PbO}$  to the phosphate glass improves the chemical stability of glass network.  $\text{Ho}^{3+}$  ions the most studied among the rare earth ions and the up conversion process of this ion in various kinds of host materials has been investigated [14-18].

The present work reports on the preparation and characterization of rare earth doped heavy metal oxide (HMO) glass systems for lasing materials. I have studied on the Optical absorption, Excitation and fluorescence spectra of  $\text{Ho}^{3+}$  doped zinc lithium lead sodalime cadmium phosphate glasses. The intensities of the transitions for the rare earth ions have been estimated successfully using the Judd-Ofelt theory, The laser parameters such as radiative probabilities(A), branching ratio ( $\beta$ ), radiative life time( $\tau_R$ ) and stimulated emission cross section( $\sigma_p$ ) are evaluated using J.O.intensity parameters( $\Omega_\lambda$ ,  $\lambda=2, 4$  and 6).

## II. EXPERIMENTAL TECHNIQUES

### A. Preparation of Glasses

The following  $\text{Ho}^{3+}$  doped phosphate glass samples  $(35-x)\text{P}_2\text{O}_5:10\text{ZnO}:10\text{Li}_2\text{O}:10\text{PbO}:10\text{CaO}:10\text{Na}_2\text{O}:15\text{CdO}: x \text{Ho}_2\text{O}_3$  (where  $x=1, 1.5$  and 2 mol%) have been prepared by melt-quenching method. Analytical reagent grade chemical used in the present study consist of  $\text{P}_2\text{O}_5$ ,  $\text{ZnO}$ ,  $\text{Li}_2\text{O}$ ,  $\text{PbO}$ ,  $\text{CaO}$ ,  $\text{Na}_2\text{O}$ ,  $\text{CdO}$  and  $\text{Ho}_2\text{O}_3$ .

They were thoroughly mixed by using an agate pestle mortar. then melted at  $1072^\circ\text{C}$  by an electrical muffle furnace for 2h., After complete melting, the melts were quickly poured in to a preheated stainless steel mould and annealed at temperature of  $250^\circ\text{C}$  for 2h to remove thermal strains and stresses. Every time fine powder of cerium oxide was used for polishing the samples. The glass samples so prepared were of good optical quality and were transparent. The chemical compositions of the glasses with the name of samples are summarized in Table 1.

Table 1.

Chemical composition of the glasses

Sample	Glass composition (mol %)
ZLLSLCP(UD)	35P <sub>2</sub> O <sub>5</sub> :10ZnO:10Li <sub>2</sub> O:10PbO:10CaO:10Na <sub>2</sub> O:15CdO
ZLLSLCP(HO1)	34P <sub>2</sub> O <sub>5</sub> :10ZnO:10Li <sub>2</sub> O:10PbO:10CaO:10Na <sub>2</sub> O:15CdO:1 Ho <sub>2</sub> O <sub>3</sub>
ZLLSLCP(HO1.5)	33.5P <sub>2</sub> O <sub>5</sub> :10ZnO:10Li <sub>2</sub> O:10PbO:10CaO:10Na <sub>2</sub> O:15CdO:1.5 Ho <sub>2</sub> O <sub>3</sub>
ZLLSLCP(HO2)	33P <sub>2</sub> O <sub>5</sub> :10ZnO:10Li <sub>2</sub> O:10PbO:10CaO:10Na <sub>2</sub> O:15CdO:2 Ho <sub>2</sub> O <sub>3</sub>

ZLLSLCP (UD) -Represents undoped Zinc Lithium Lead Sodalime Cadmium Phosphate glass specimens  
 ZLLSLCP (HO)-Represents Ho<sup>3+</sup> doped Zinc Lithium Lead Sodalime Cadmium Phosphate glass specimens

### III. THEORY

#### A. Oscillator Strength

The intensity of spectral lines are expressed in terms of oscillator strengths using the relation [19].

$$f_{\text{expt.}} = 4.318 \times 10^{-9} \int \epsilon(\nu) d\nu \tag{1}$$

where,  $\epsilon(\nu)$  is molar absorption coefficient at a given energy  $\nu$  (cm<sup>-1</sup>), to be evaluated from Beer–Lambert law.

Under Gaussian Approximation, using Beer–Lambert law, the observed oscillator strengths of the absorption bands have been experimentally calculated [20], using the modified relation:

$$P_m = 4.6 \times 10^{-9} \times \frac{1}{cl} \log \frac{I_0}{I} \times \Delta\nu_{1/2} \tag{2}$$

where  $c$  is the molar concentration of the absorbing ion per unit volume,  $l$  is the optical path length,  $\log I_0/I$  is optical density and  $\Delta\nu_{1/2}$  is half band width.

#### B. Judd-Ofelt Intensity Parameters

According to Judd [21] and Ofelt [22] theory, independently derived expression for the oscillator strength of the induced forced electric dipole transitions between an initial  $J$  manifold  $|4f^N(S, L) J\rangle$  level and the terminal  $J'$  manifold  $|4f^N(S', L') J'\rangle$  is given by:

$$\frac{8\pi^2 m c \bar{\nu}}{3h(2J+1)n} \left[ \frac{(n^2+2)^2}{9} \right] \times S(J, J') \tag{3}$$

Where,

the line strength  $S(J, J')$  is given by the equation

$$S(J, J') = e^2 \sum_{\lambda=2, 4, 6} \Omega_{\lambda} \langle 4f^N(S, L) J || U^{(\lambda)} || 4f^N(S', L') J' \rangle^2 \tag{4}$$

In the above equation  $m$  is the mass of an electron,  $c$  is the velocity of light,  $\bar{\nu}$  is the wave number of the transition,  $h$  is Planck's constant,  $n$  is the refractive index,  $J$  and  $J'$  are the total angular momentum of the initial and final level respectively,  $\Omega_{\lambda}$  ( $\lambda=2, 4$  and  $6$ ) are known as Judd-Ofelt intensity.

#### C. Radiative Properties

The  $\Omega_{\lambda}$  parameters obtained using the absorption spectral results have been used to predict radiative properties such as spontaneous emission probability ( $A$ ) and radiative life time ( $\tau_R$ ), and laser parameters like fluorescence branching ratio ( $\beta_R$ ) and stimulated emission cross section ( $\sigma_p$ ).

The spontaneous emission probability from initial manifold  $|4f^N(S', L') J'\rangle$  to a final manifold  $|4f^N(S, L) J\rangle$  is given by:

$$A[(S', L') J'; (S, L) J] = \frac{64 \pi^2 \bar{\nu}^3}{3h(2J'+1)} \left[ \frac{n(n^2+2)^2}{9} \right] \times S(J', \bar{J}) \tag{5}$$

Where,  $S(J', J) = e^2 [\Omega_2 || U^{(2)} ||^2 + \Omega_4 || U^{(4)} ||^2 + \Omega_6 || U^{(6)} ||^2]$

The fluorescence branching ratio for the transitions originating from a specific initial manifold  $|4f^N(S', L') J' \rangle$  to a final many fold  $|4f^N(S, L) J \rangle$  is given by

$$\beta [(S', L') J'; (S, L) J] = \frac{A[(S', L') J'; (S, L) J]}{\sum_{S, L, J} A[(S', L') J'; (S, L) J]} \quad (6)$$

where, the sum is over all terminal manifolds.

The radiative life time is given by

$$\tau_{rad} = \frac{1}{\sum_{S, L, J} A[(S', L') J'; (S, L) J]} = A_{Total}^{-1} \quad (7)$$

where, the sum is over all possible terminal manifolds. The stimulated emission cross-section for a transition from an initial manifold  $|4f^N(S', L') J' \rangle$  to a final manifold  $|4f^N(S, L) J \rangle$  is expressed as

$$\sigma_p(\lambda_p) = \left[ \frac{\lambda_p^4}{8\pi c n^2 \Delta\lambda_{eff}} \right] \times A[(S', L') J'; (S, L) J] \quad (8)$$

where,  $\lambda_p$  the peak fluorescence wavelength of the emission band and  $\Delta\lambda_{eff}$  is the effective fluorescence line width.

#### D. Nephelauxetic Ratio ( $\beta'$ ) and Bonding Parameter ( $b^{1/2}$ )

The nature of the R-O bond is known by the Nephelauxetic Ratio ( $\beta'$ ) and Bonding Parameters ( $b^{1/2}$ ), which are computed by using following formulae [23, 24]. The Nephelauxetic Ratio is given by

$$\beta' = \frac{\nu_g}{\nu_a} \quad (9)$$

where,  $\nu_a$  and  $\nu_g$  refer to the energies of the corresponding transition in the glass and free ion, respectively. The value of bonding parameter ( $b^{1/2}$ ) is given by

$$b^{1/2} = \left[ \frac{1-\beta'}{2} \right]^{1/2} \quad (10)$$

### IV. RESULT AND DISCUSSION

#### A. XRD Measurement

Figure 1 presents the XRD pattern of the sample contain – P<sub>2</sub>O<sub>5</sub> which is show no sharp Bragg's peak, but only a broad diffuse hump around low angle region. This is the clear indication of amorphous nature within the resolution limit of XRD instrument.

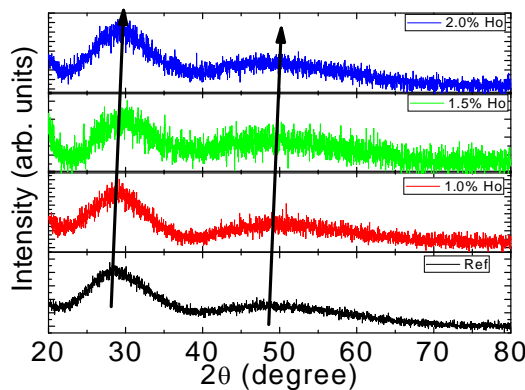


Fig. 1 X-ray diffraction pattern of ZLLSLCP (HO) Glasses.

**B. Up conversion Emission Mechanism**

Up-conversion emission mechanism for the zinc lithium lead sodalime cadmium phosphate glasses are schematically depicted as fig.2

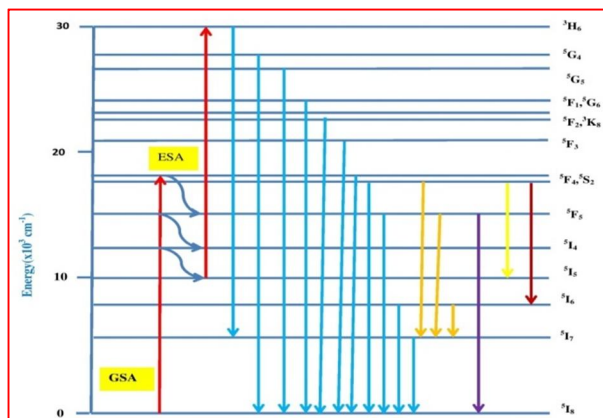


Fig. (2) Upconversion emission Mechanism.

**C. Absorption Spectrum**

The absorption spectra of Ho<sup>3+</sup> doped ZLLSLCP glass specimens have been presented in Figure 3 in terms of optical density versus wavelength. Twelve absorption bands have been observed from the ground state <sup>5</sup>I<sub>8</sub> to excited states <sup>5</sup>I<sub>5</sub>, <sup>5</sup>I<sub>4</sub>, <sup>5</sup>F<sub>5</sub>, <sup>5</sup>F<sub>4</sub>, <sup>5</sup>F<sub>3</sub>, <sup>3</sup>K<sub>8</sub>, <sup>5</sup>G<sub>6</sub>, (<sup>5</sup>G, <sup>3</sup>G)<sub>5</sub>, <sup>5</sup>G<sub>4</sub>, <sup>5</sup>G<sub>2</sub>, <sup>5</sup>G<sub>3</sub>, and <sup>3</sup>F<sub>4</sub> for Ho<sup>3+</sup> doped ZLLSLCP glasses.

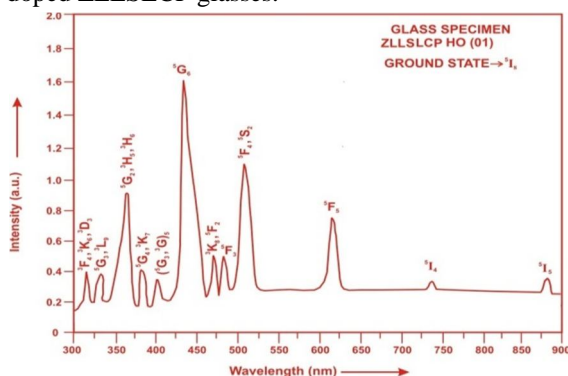


Fig. (3) Absorption spectrum of ZLLSLCP HO (01) glass.

The experimental and calculated oscillator strength for Ho<sup>3+</sup> ions in ZLLSLCP glasses are given in **Table 3**.

Table 3: Measured and calculated oscillator strength ( $P_m \times 10^{+6}$ ) of Ho<sup>3+</sup> ions in ZLLSLCP glasses.

Energy level from <sup>5</sup> I <sub>8</sub>	Glass ZLLSLCP (HO01)		Glass ZLLSLCP (HO1.5)		Glass ZLLSLCP (HO02)	
	P <sub>exp.</sub>	P <sub>cal.</sub>	P <sub>exp.</sub>	P <sub>cal.</sub>	P <sub>exp.</sub>	P <sub>cal.</sub>
<sup>5</sup> I <sub>5</sub>	0.40	0.24	0.43	0.24	0.39	0.24
<sup>5</sup> I <sub>4</sub>	0.05	0.02	0.04	0.02	0.03	0.02
<sup>3</sup> F <sub>5</sub>	3.68	2.81	3.65	2.79	3.61	2.76
<sup>3</sup> F <sub>4</sub>	4.72	4.37	4.69	4.33	4.65	4.29
<sup>3</sup> F <sub>3</sub>	1.55	2.43	1.52	2.41	1.48	2.39
<sup>3</sup> K <sub>8</sub>	1.48	1.98	1.45	1.96	1.41	1.93
<sup>5</sup> G <sub>6</sub>	24.86	26.84	23.72	23.72	24.65	22.67
( <sup>5</sup> G, <sup>3</sup> G) <sub>5</sub>	3.82	1.70	3.78	1.68	3.75	1.66
<sup>5</sup> G <sub>4</sub>	0.07	0.61	0.06	0.60	0.05	0.59
<sup>5</sup> G <sub>2</sub>	5.86	5.31	5.83	5.11	5.79	4.91
<sup>5</sup> G <sub>3</sub>	1.53	1.39	1.50	1.37	1.46	1.34
<sup>3</sup> F <sub>4</sub>	1.44	4.18	1.41	4.13	1.38	4.09
r.m.s. deviation	±1.1018		±1.1030		±1.1077	

Computed values of  $F_2$ , Lande' parameter ( $\xi_{4f}$ ), Nephelauxetic ratio ( $\beta'$ ) and bonding parameter ( $b^{1/2}$ ) for  $\text{Ho}^{3+}$  ions in ZLLSLCP glass specimen are given in Table 3.

Table 3:  $F_2, \xi_{4f}, \beta'$  and  $b^{1/2}$  parameters for Holmium doped glass specimen.

Glass Specimen	$F_2$	$\xi_{4f}$	$\beta'$	$b^{1/2}$
$\text{Ho}^{3+}$	358.82	1258.16	0.9337	0.1821

In the Zinc Lithium Lead Sodalime Cadmium Phosphate glasses (ZLLSLCP)  $\Omega_2, \Omega_4$  and  $\Omega_6$  parameters decrease with the increase of x from 1 to 2 mol%. The order of magnitude of Judd-Ofelt intensity parameters is  $\Omega_2 > \Omega_6 > \Omega_4$  for all the glass specimens. The spectroscopic quality factor ( $\Omega_4 / \Omega_6$ ) related with the rigidity of the glass system has been found to lie between 0.603 and 0.608 in the present glasses.

The values of Judd-Ofelt intensity parameters are given in Table 4.

Table 4: Judd-Ofelt intensity parameters for  $\text{Ho}^{3+}$  doped ZLLSLCP glass specimens.

Glass Specimen	$\Omega_2(\text{pm}^2)$	$\Omega_4(\text{pm}^2)$	$\Omega_6(\text{pm}^2)$	$\Omega_4 / \Omega_6$
ZLLSLCP (HO01)	5.817	1.302	2.140	0.6084
ZLLSLCP (HO1.5)	5.506	1.282	2.125	0.6033
ZLLSLCP (HO02)	5.212	1.269	2.104	0.6031

#### D. Excitation Spectrum

The Excitation spectrum of ZLLSLCP (HO 01) glass has been presented in Figure 4 in terms of Excitation Intensity versus wavelength. The excitation spectrum was recorded in the spectral region 325–525 nm fluorescence at 545nm having different excitation band centered at 349,419, 452, 473and 486 nm are attributed to the  $^5G_3, (^5G, ^3G)_5, ^5G_6, ^3K_8$  and  $^5F_3$  transitions, respectively. The highest absorption level is  $^5G_6$  and is at 452nm. So this is to be chosen for excitation wavelength.

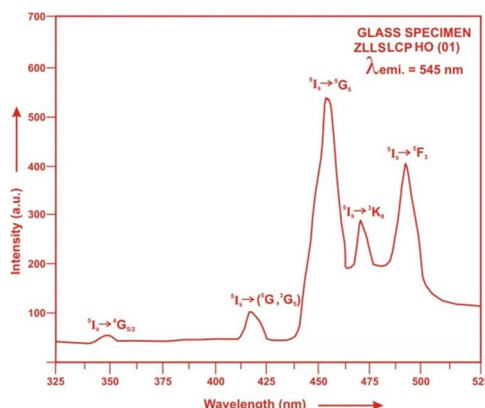


Fig. (4) Excitation spectrum of ZLLSLCP HO (01) glass.

E. Fluorescence Spectrum

The fluorescence spectrum of  $\text{Ho}^{3+}$  doped in zinc lithium lead sodalime cadmium phosphate glass is shown in Figure 5. There are eleven broad bands observed in the Fluorescence spectrum of  $\text{Ho}^{3+}$  doped zinc lithium lead sodalime cadmium phosphate glass. The wavelengths of these bands along with their assignments are given in Table 5. The peak with maximum emission intensity appears at 2035 nm and corresponds to the ( $^5\text{I}_7 \rightarrow ^5\text{I}_8$ ) transition.

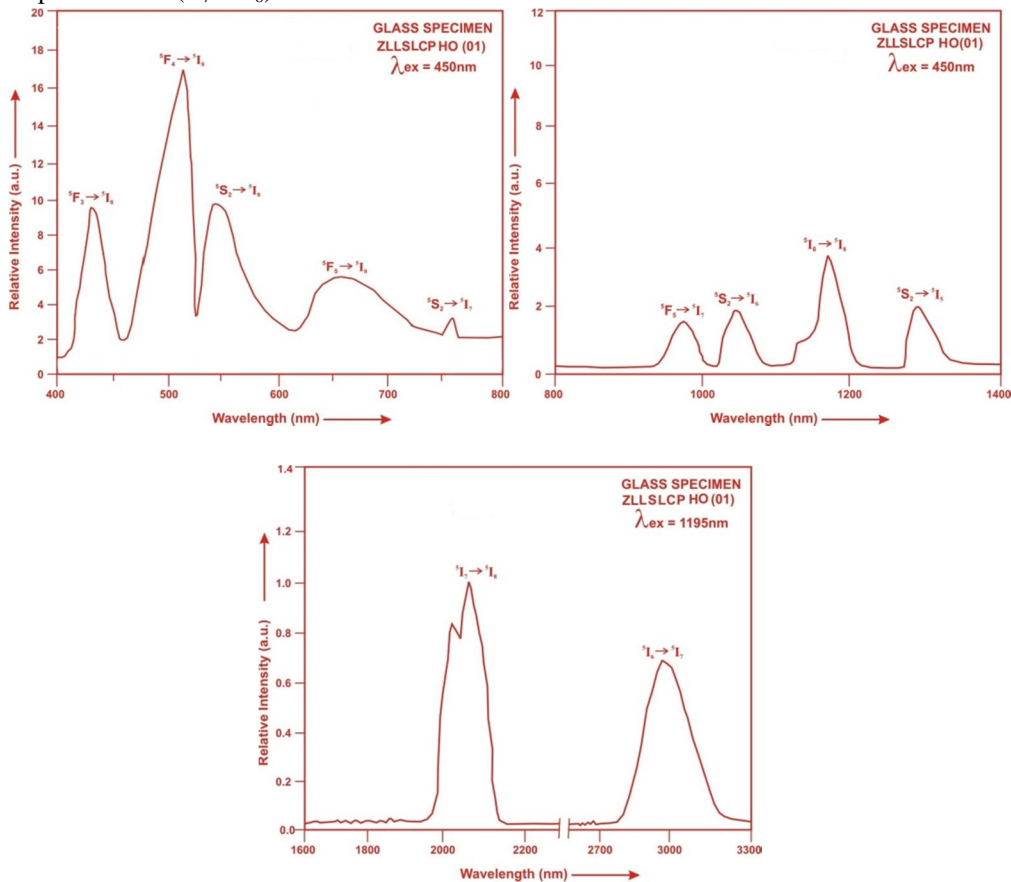


Fig. (5). Fluorescence spectrum of ZLLSLCP HO (01) glass.

Table5: Emission peak wave lengths ( $\lambda_p$ ),radiative transition probability ( $A_{rad}$ ),branching ratio ( $\beta$ ),stimulated emission cross-section ( $\sigma_p$ ) and radiative life time( $\tau_R$ ) for various transitions in  $\text{Ho}^{3+}$  doped ZLLSLCP glasses.

Transition	ZLLSLCP (HO 01)					ZLLSLCP (HO 1.5)				ZLLSLCP (HO 02)			
	$\lambda_{max}$ (nm)	$A_{rad}(s^{-1})$	$\beta$	$\sigma_p (10^{-20} cm^2)$	$\tau_R(\mu s)$	$A_{rad}(s^{-1})$	$\beta$	$\sigma_p (10^{-20} cm^2)$	$\tau_R (\mu s)$	$A_{rad}(s^{-1})$	$\beta$	$\sigma_p (10^{-20} cm^2)$	$\tau_R (10^{-20} cm^2)$
$^5F_3 \rightarrow ^5I_8$	435	4421.05	0.2476	0.599	5601.28	4401.73	0.2480	0.585	5634.16	4366.81	0.2480	0.570	5680.07
$^5F_4 \rightarrow ^5I_8$	501	7060.83	0.3955	1.237		7017.17	0.3954	1.213		6961.25	0.3954	1.187	
$^5S_2 \rightarrow ^5I_8$	555	1846.68	0.1034	0.434		1837.34	0.1035	0.427		1822.76	0.1035	0.416	
$^5F_5 \rightarrow ^5I_8$	652	2005.98	0.1124	0.729		1990.59	0.1122	0.714		1974.64	0.1122	0.698	
$^5S_2 \rightarrow ^5I_7$	761	1406.48	0.0788	1.119		1399.37	0.0788	1.100		138.83	0.0789	1.073	
$^5F_5 \rightarrow ^5I_7$	995	464.43	0.0260	1.194		459.27	0.0259	1.166		453.97	0.0258	1.131	
$^5I_6 \rightarrow ^5I_8$	1032	214.79	0.0120	0.692		213.54	0.0120	0.678		211.84	0.0120	0.660	
$^5S_2 \rightarrow ^5I_5$	1195	245.24	0.0138	1.212		243.57	0.0137	1.189		241.31	0.0137	1.164	
$^5S_2 \rightarrow ^5I_6$	1310	65.44	0.0037	0.623		65.08	0.0037	0.610		64.58	0.0037	0.592	
$^5I_7 \rightarrow ^5I_8$	2035	97.37	0.0055	4.653		96.65	0.0054	4.557		95.71	0.0054	4.453	
$^5I_6 \rightarrow ^5I_7$	2925	24.78	0.0014	3.907		24.55	0.0014	3.823		24.27	0.0014	3.728	

## V. CONCLUSION

In the present study, the glass samples of composition  $(35x)\text{P}_2\text{O}_5:10\text{ZnO}:10\text{Li}_2\text{O}:10\text{PbO}:10\text{CaO}:10\text{Na}_2\text{O}:15\text{CdO}:x\text{Ho}_2\text{O}_3$ , (where  $x = 1, 1.5$  and  $2$  mol %) have been prepared by melt-quenching method. The value of stimulated emission cross-section ( $\sigma_p$ ) is found to be maximum for the transition ( $^5\text{I}_7 \rightarrow ^5\text{I}_8$ ) for glass ZLLSLCP (HO 01), suggesting that glass ZLLSLCP (HO 01) is better compared to the other two glass systems ZLLSLCP (HO1.5) and ZLLSLCP (HO 02). The large stimulated emission cross section in bismuth borate glasses suggests the possibility of utilizing these systems as laser materials.

## REFERENCES

- [1] Alqarni, A. S., Hussin, R., Alamri, S.N., Ghoshal, S.K. (2020). Tailored structures and dielectric traits of holmium ion-doped zinc-sulpho-boro-phosphate glass ceramics. *Ceramics International*, 46(3):3282-3291
- [2] Nasser, K., Aseev, V., Ivanov, S., Ignatiev, A. and Nikonov, N. (2019). Optical spectroscopic properties and Judd-ofelt analysis of  $\text{Nd}^{3+}$  doped photo thermo refractive glass. *J. lumen*. 213, 255-262.
- [3] Nayab Rasool, S.K., Rama Moorthy, L. and Jayasankar, C.K. (2013). Spectroscopic investigation of  $\text{Sm}^{3+}$  doped phosphate based glasses for reddish orange emission. *Optical Communication*, 3115, 156-165.
- [4] Gokce, M., Kocyigit, D. (2021). Spectroscopic investigations of  $\text{Dy}^{3+}$  doped borogermanate glasses for laser and WLED applications. *Opt. Mater.* 89, 568-575.
- [5] Karki, S., Kesavulu, C.R., Kim, H.J., Kaewkho, J., Chanthima, N., Kothan, S., Kaewjaeng, S. (2019). Physical, optical and luminescence properties of the  $\text{Dy}^{3+}$  doped barium borophosphate glasses. *J. Noncryst. Solids*, 521, 119483.
- [6] Kaur, R., Rakesh, R.B., Mhatre, S.G., Bhatia, V., Kumar, D., Singh, H., Singh, S.P. and Kumar, A. (2021). Physical, optical, structural and thermoluminescence behavior of borosilicate glasses doped with trivalent neodymium ions. *Opt. Mater.* 117, 1-13.
- [7] Shoab, N., Chanthima, N., Rooh, G., Rajaramkrishna, R. and Kaewkhao, J. (2019). Physical and luminescence properties of rare earth doped phosphate glasses for solid state lighting applications. *Thai Int. Res.* 14, 20-26.
- [8] Kashif, I., Ratep, A. (2021). Judd-Ofelt and luminescence study of Dysprosium-doped lithium borosilicate glasses for lasers and w-LEDs. *Bol. Soc. Esp. Ceram. Vidr.* 61, 1-12.
- [9] Liu, L., Shi, Z., Song, Q., Li, D., Li, N., Xue, Y., Xu, J., Xu, J., Wang, and Xu, X. (2020). Judd-Ofelt analysis and spectroscopic study of  $\text{Tb}:\text{CaF}_2$  and  $\text{Tb}/\text{Pr}:\text{CaF}_2$  co-doped single crystals. *Opt. Mater.* 108, 1-5.
- [10] Marzouk, M.A. and Elbatal, H.A. (2021). Investigation of photoluminescence and spectroscopic properties of  $\text{Sm}^{3+}$  doped heavy phosphate glasses before and after gamma irradiation. 70, 1-10.
- [11] Smith, C.E., Brow, R.K. (2014). The properties and structure of zinc magnesium phosphate glasses. *J. Non-Cryst. Solids*. 390, 51-58
- [12] Ehrt, D., Ebeling, P., Natura, U. (2000). UV Transmission and radiation induced defects in phosphate and fluoride-phosphate glasses. *J. Non-Cryst. Solids*, 263, 240-250.
- [13] Devi, R. and Jayasankar, C. K. (1995). Optical properties of  $\text{Nd}^{3+}$  ions in lithium borate glasses. *Materials chemistry and phys.* 42, 106-119.
- [14] Suresh, K., Jayasankar, C.K. (2019). Conversion of blue-green photon into NIR photons in  $\text{Ho}^{3+}/\text{Yb}^{3+}$  co-doped zinc tellurite glasses. *J. Alloys-Compd.* 788, 1048-1055.
- [15] Mahamuda, Sk., Swapna, K., Packiyaraj, P., Rao, A.S. and Prakash, G.V. (2013). Visible red, NIR and Mid-IR emission studies of  $\text{Ho}^{3+}$  doped Zinc Alumino Bismuth Borate Glasses. *Opt. Mater.* 36, 362-371.
- [16] Meena, S.L. (2020). Spectral and Thermal Properties of  $\text{Ho}^{3+}$  Doped in Zinc Lithium Alumino Antimony Borophosphate Glasses. *Int. J. Scie. Dev. Res.* 5, 127-133.
- [17] Kowalska, K., Kuwik, M., Pisanska, J. and Pisanski, W.A. (2022). Near-IR Luminescence of Rare-Earth Ions ( $\text{Er}^{3+}$ ,  $\text{Pr}^{3+}$ ,  $\text{Ho}^{3+}$ ,  $\text{Tm}^{3+}$ ) in Titanate-Germanate Glasses under Excitation of  $\text{Yb}^{3+}$ . 15, 1-13.
- [18] Cai, M., Zhou, B., Wang, F., Tian, Y., Zhou, J., Xu, S., Zhang, J. (2015). Highly efficient mid-infrared 2  $\mu\text{m}$  emission in  $\text{Ho}^{3+}/\text{Yb}^{3+}$ -codoped germanate glass. *Opt. Mater. Express*. 5, 1431-1439.
- [19] Gorler-Walrand, C. and Binnemans, K. (1988). Spectral Intensities of f-f Transition. In: Gshneidner Jr., K.A. and Eyring, L., Eds., *Handbook on the Physics and Chemistry of Rare Earths*, Vol. 25, Chap. 167, North-Holland, Amsterdam, 101-264.
- [20] Sharma, Y.K., Surana, S.S.L. and Singh, R.K. (2009) Spectroscopic Investigations and Luminescence Spectra of  $\text{Sm}^{3+}$  Doped Soda Lime Silicate Glasses. *Journal of Rare Earths*, 27, 773-780.
- [21] Judd, B.R. (1962). Optical Absorption Intensities of Rare Earth Ions. *Physical Review*, 127, 750-761.
- [22] Ofelt, G.S. (1962). Intensities of Crystal Spectra of Rare Earth Ions. *The Journal of Chemical Physics*, 37, 511.
- [23] Sinha, S.P. (1983). Systematics and properties of lanthanides, Reidel, Dordrecht. 1-8.
- [24] Krupke, W.F. (1974). *IEEE J. Quantum Electron QE*, 10, 450





10.22214/IJRASET



45.98



IMPACT FACTOR:  
7.129



IMPACT FACTOR:  
7.429



# INTERNATIONAL JOURNAL FOR RESEARCH

IN APPLIED SCIENCE & ENGINEERING TECHNOLOGY

Call : 08813907089  (24\*7 Support on Whatsapp)